구형좌표계에서 음향 홀로그래피의 적용
The implementation of spherical acoustical holography

조용성*, J. Stuart Bolton**, 김용조***

Yong Thung Cho*, J. Stuart Bolton**, and Yong-Joe Kim***

Key Words: 구형음향홀로그래피(spherical acoustical holography), 파워필터링(power filtering), 소음원식별(noise source identification)

ABSTRACT

In this article, spatial filtering procedures with application to spherical acoustical holography are discussed. Planar and cylindrical holography are the most widely used amongst the various nearfield acoustical holography techniques. However, when the geometry of a source is similar to a sphere, spherical holography may yield better results than other types of holography since there are no errors due to truncation of the sound field in the spherical case. Spatial filtering affects the accuracy of spherical acoustical holography critically, especially in the case of backward projection. Thus spatial filtering is essential for successful application of spherical holography. In the present work, various filtering methods were evaluated in simulations made using sound pressure fields of various types and with different levels of random spatial noise. It was found that a procedure based on eliminating spherical harmonic coefficients that contribute insignificantly to the total sound power of the source gave the best results on average of the different procedures considered here. Spherical holography procedures were also verified experimentally. Reliable results were obtained using the power filtering algorithm. Thus it was concluded that spherical holography combined with power filtering may prove to be a useful tool for noise source identification.

1. Introduction

Two-microphone intensity probes can be used to determine the sound energy flow near a source but they can be used to measure the vector intensity only at a single point in space. Thus, detailed intensity measurements on a surface enclosing a noise source may be time consuming, and if the intensities are measured only on a single surface, the results may be misleading in the presence of a circulating intensity, for example.

In contrast, by implementing an acoustical holography procedure, the complete acoustical properties of a three-dimensional sound field can be calculated from a knowledge of the sound pressure measured on an appropriate two-dimensional surface: i.e., the hologram surface. When operated on with appropriate propagators, measurements of pressure on a two-dimensional surface can be projected either as pressure or acoustic particle velocity to a sequence of finely spaced surfaces close to a source, which thus makes it possible to create a detailed, three-dimensional visualization of the source's sound field.

There are several types of holography procedures in use at present: i.e., nearfield planar, cylindrical, spherical, and boundary element. These procedures differ primarily in the geometry of the measurement surface: i.e., the hologram surface. All four types of holography start from the solution of the homogeneous wave equation. By use of an appropriate Green's function, or propagator, forward projections can be made to visualize the sound field away from the sound source. Conversely, the inverse of the Green's function, or propagator, can be used to perform backward projections of the sound field in order to visualize the sound field close to the sound source.

Planar holography was originally introduced by Maynard et al. [1] and was extended to the case of multiple incoherent sources by Hald and Ginn [2]. This style of holography has to-date been the most widely

* Purdue University, USA
E-mail : choy@purdue.edu
Tel : +1-765-494-2146, Fax : +1-765-494-0787

** Purdue University

*** Purdue University

used. But it is not possible, or at least is not effective, to implement planar holography for some source geometries. The surfaces of some sources, for example, the surfaces of submarines, aircraft fuselage interiors, piping systems, and circular ducts conform much more closely to a cylindrical than a planar surface [3-5]. Similarly, there are sources such as small refrigeration compressors that can conveniently be enclosed in spherical surfaces [6,7]. For this reason, spherical holography was the focus of the current work. Note that a boundary element implementation of holography may be used when the source may not conveniently be enclosed by a spherical surface [9].

Weinreich and Arnold [8] were the first to develop procedures for performing spherical holography experiments. Spherical holography differs from planar and cylindrical holography in that the measurement surface completely encloses the source. The measured pressure distribution is then approximated as a finite sum of spherical harmonics with appropriate coefficients, which has the effect of decomposing the sound field on the hologram surface into spherical wave components each of which has known radial propagation characteristics. The decomposed sound field may then be propagated to another radius on a component-by-component basis, and then reassembled to create the sound field on a reconstruction surface [5-8,10-12]. Note that a more extensive description of the present results is available elsewhere [12].

2. ANALYTICAL FORMULATION OF SPHERICAL HOLOGRAPHY

2.1 Introduction

A summary of the analytical formulation of spherical holography is first presented in this section. In essence, the expression representing spherical wave radiation from a sound source consists of summations of spherical Hankel functions multiplied by spherical harmonics. By appropriately manipulating the equations governing spherical wave radiation from sound sources, it is possible to calculate the sound pressure, particle velocity, acoustic intensity, and sound power radiated from the source at arbitrary distances from the spherical hologram surface.

2.2 Summary of Analytical Formulation

Spherical waves radiating from sources enclosed within a spherical surface, S, can be expressed as [10]

$$p(r,\theta,\phi,\omega)=\sum_{n=0}^{+\infty}h_n(kr)\sum_{m=0}^{n}[A_{nm}Y_{nm}^{+}(\theta,\phi)+B_{nm}Y_{nm}^{-}(\theta,\phi)], \tag{1}$$

In Eq. (1), $p(r,\theta,\phi,\omega)$ is the pressure at the location (r,θ,ϕ) at the angular frequency ω, $h_n(kr)$ is the spherical Hankel function of order n, $k=\omega/c$ where c is the sound speed, $Y_{nm}^{+}(\theta,\phi)$ and $Y_{nm}^{-}(\theta,\phi)$ are the spherical harmonics (i.e., modal functions on a sphere), A_{nm} and B_{nm} are the spherical harmonic coefficients, and θ and ϕ are the polar and azimuthal angles, respectively, on the spherical measurement surface. The coordinate system used here is illustrated in Fig. 1.

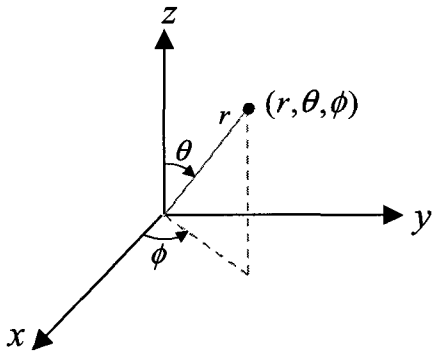

Fig. 1 Coordinates used for spherical acoustic holography.

Note that the spherical Hankel function, $h_n(kr)$, that appears in Eq. (1) implicitly contains the exponential e^{ikr}, which corresponds to outward sound radiation when using an $e^{-i\omega t}$ time convention.

The spherical harmonic functions Y_{nm}^{+} and Y_{nm}^{-} can be expressed in terms of Legendre functions [10]: i.e.,

$$Y_{nm}^{+}(\theta,\phi)=\cos(m\phi)\sin^m(\theta)\frac{d^mP_n(\cos(\theta))}{d(\cos(\theta))^m}, \tag{2}$$

and

$$Y_{nm}^{-}(\theta,\phi)=\sin(m\phi)\sin^m(\theta)\frac{d^mP_n(\cos(\theta))}{d(\cos(\theta))^m}, \tag{3}$$

where P_n is the Legendre function of order n. By using the orthogonal properties of the spherical harmonics, the coefficients A_{nm} and B_{nm} can be expressed as follows [10]:

$$A_{nm}=\frac{(2n+1)}{4\pi}\varepsilon_m\frac{(n-m)!}{(n+m)!}\frac{1}{h_n(kr)} \times\int_0^{2\pi}d\phi\int_0^{\pi}p(r,\theta,\phi,\omega)Y_{nm}^{+}(\theta,\phi)\sin(\theta)d\theta, \tag{4}$$

$$B_{nm}=\frac{(2n+1)}{4\pi}\varepsilon_m\frac{(n-m)!}{(n+m)!}\frac{1}{h_n(kr)} \times\int_0^{2\pi}d\phi\int_0^{\pi}p(r,\theta,\phi,\omega)Y_{nm}^{-}(\theta,\phi)\sin(\theta)d\theta, \tag{5}$$

where

$$\varepsilon_m = \begin{cases} 1 & for\ m = 0 \\ 2 & for\ m \geq 1. \end{cases}$$

Thus, when the pressure distribution is measured at a hologram surface located at $r = r_0$, the spherical harmonic coefficients, A_{nm} and B_{nm}, can be calculated from Eqs. (4) and (5). The pressure distribution at a reconstruction surface, located at $r = r_1$, either closer to or farther away from the sound source than the measurement surface, can be calculated by substituting into Eq. (1) the radius of the reconstruction surface, $r = r_1$, and the spherical harmonic coefficients A_{nm} and B_{nm} calculated from the measured pressure distribution at $r = r_0$.

It is possible to calculate the particle velocity, acoustic intensity, and radiated sound power in addition to the sound pressure by using acoustic holography. Note that from Euler's equation, the radial particle velocity, u_r, can be expressed in terms of the radial pressure gradient [10]: i.e.,

$$u_r(r,\theta,\phi,\omega) = \frac{-i}{\rho_0 \omega} \frac{\partial p(r,\theta,\phi,\omega)}{\partial r}, \tag{6}$$

where ρ_0 is the density. Since terms other than $h_n(kr)$ in Eq. (1) are independent of r, the partial derivative of the sound pressure in the radial direction can be calculated by differentiating only the $h_n(kr)$ term with respect to r. As a result, the radial particle velocity can be expressed as

$$u_r(r,\theta,\phi,\omega) = \frac{-i}{\rho_0 c} \sum_{n=0}^{+\infty} \frac{1}{2n+1} \left[n h_{n-1}(kr) - (n+1) h_{n+1}(kr) \right] \times \sum_{m=0}^{n} \left[A_{nm} Y_{nm}^{+}(\theta,\phi) + B_{nm} Y_{nm}^{-}(\theta,\phi) \right]. \tag{7}$$

The radial, active acoustic intensity, $I_r(r,\theta,\phi,\omega)$, can be calculated by using the acoustic pressure and radial acoustic particle velocity as

$$I_r(r,\theta,\phi,\omega) = \frac{1}{2} \mathrm{Re}\left\{ p(r,\theta,\phi,\omega) u_r^*(r,\theta,\phi,\omega) \right\}, \tag{8}$$

where the superscript, *, denotes the complex conjugate operation. Finally, the sound power, W, radiated from the sound source can be calculated by integrating the sound intensity over a spherical surface: i.e.,

$$W = \int_0^{2\pi} \int_0^{\pi} I_r(r,\theta,\phi,\omega) r^2 \sin(\theta) d\theta\, d\phi. \tag{9}$$

3. SPATIAL FILTERING

3.1 Introduction

Owing to positioning errors, sound scattering from the measurement apparatus, etc., the pressure on the hologram surface is inevitably corrupted by spatial noise. This noise causes the evaluation of the spherical harmonic coefficients to be inaccurate: i.e., the coefficients are "noisy".

The noisy high order field components, in particular, are amplified more than the low order components of the measured pressure during backward projections. The result may be that the pressure field is completely dominated by noisy higher order terms after backward projection. Thus, the spatial filtering of noisy, measured pressures before or during backward projection is the most important step in ensuring the stability and accuracy of spherical acoustical holography.

In the present work, ten different filtering methods were compared. These ten filtering methods were applied to one of: the spherical harmonic coefficients, the radiated sound power, the magnitude of the measured pressure, the acoustical transfer matrix relating the pressure on the hologram surface to that on the reconstruction surface [12], or combinations of these.

3.2 Filtering Methods

In this section, the various filtering procedures are described. These various filtering procedures were applied to sound fields generated by arbitrary sound sources (comprising combinations of monopoles) having significant higher order terms. In addition, random noise was superimposed on the simulated pressure fields since it was found that the sound source type and the signal-to-noise ratio affected the relative performance of the filtering methods. The performance of the various filtering procedures was then quantified in terms of the mean square error after projection. It has been found that a so-called power filtering procedure usually resulted in the smallest, or nearly the smallest, projection error.

3.2.1 Coefficient Filtering

First, the spherical harmonic coefficients were evaluated from the measured pressure. Then, the magnitude of each harmonic coefficient was compared with the spherical harmonic coefficient having the largest magnitude. When the value of a coefficient was smaller than the maximum by a certain level, its value was set to zero in the reconstruction process: otherwise the value of the coefficients was left unchanged. Typically, coefficients were eliminated when they were more than 20 dB to 30 dB smaller than the maximum coefficient.

3.2.2 Power Filtering

In this procedure, the sound power associated with each spherical harmonic coefficient was compared with the maximum sound power associated with any of the spherical harmonic coefficients. When the sound power associated with a particular spherical harmonic coefficient was smaller than the maximum sound power component by a certain amount, that coefficient was set

to zero in the reconstruction process.

Note that by substituting Eqs. (1), (7), and (8) into Eq. (9), the radiated sound power, W, can be expressed in terms of the spherical harmonic coefficients, A_{nm} and B_{nm}: i.e.,

$$W = \frac{\pi}{\rho_0 c k^2} \sum_{n=0}^{\infty} \sum_{m=0}^{\infty} \left(|A_{nm}|^2 + |B_{nm}|^2 \right) \frac{1}{2n+1} \frac{(n+m)!}{(n-m)!}. \quad (10)$$

By using the latter expression, the contribution of each (n,m) component to the sound power can be identified.

3.2.3 Pressure Filtering

In this procedure, the sound pressure and its spatial average were calculated using each spherical harmonic coefficient. Then, the spatially-averaged pressure magnitude associated with each spherical harmonic coefficient was compared with the maximum value associated with any of the spherical harmonic coefficients. When the spatially-averaged pressure associated with a particular spherical harmonic coefficient was smaller than the maximum by a certain level, the particular coefficient was set to zero: otherwise the value of the coefficients was left unchanged.

3.2.4 Spherical Harmonic Coefficient Truncation

Spherical harmonic coefficient truncation was the simplest filtering method considered and it was found to work moderately well. The amplification in the back projection procession is controlled by the order of the spherical Hankel function, n. Therefore in this procedure, all coefficients having n larger than a certain value were eliminated from the reconstruction process. All coefficients having n equal to or smaller than the cut off value were retained in the reconstruction process regardless of the magnitude.

3.2.5 Power Filtering Truncation

Power filtering truncation is a combination of power filtering and spherical harmonic coefficient truncation. That is, after finding the highest significant order n based on the power filtering procedure, terms of order $n+1$ and above were eliminated before reconstruction.

3.2.6 Coefficient Filtering Truncation

This procedure is a combination of coefficient filtering and spherical harmonic coefficient truncation. That is, after finding the highest order n of nonzero terms to be retained on the basis of coefficient filtering, all coefficients having n higher than that value were eliminated.

3.2.7 Pressure Filtering Truncation

Here the pressure filtering and spherical harmonic coefficient truncation procedures were combined. Thus, after finding the highest order nonzero terms by using the pressure filtering procedure, pressure filtering truncation consists simply of limiting the highest order n to the value found from the pressure filtering procedure while reconstructing the pressure.

3.2.8 SVD Filtering without Area Weighting

The SVD filtering without area weighting procedure is one in which a singular value decomposition of the hologram pressure matrix is first performed. The singular values of the pressure matrix are then truncated at a certain level to remove high order spatial components from the pressure field before the pressure is projected. This procedure worked best among the filtering methods involving SVD, but did not compare well with other methods such as power filtering or pressure filtering.

3.2.9 SVD Filtering with Area Weighting

The SVD filtering with area weighting procedure is exactly the same procedure as SVD without area weighting except that the pressure is area weighted to reflect the area of the measurement sphere over which it applies before the SVD is performed.

3.2.10 SVD of Transfer Matrix

The final procedure, SVD of the transfer matrix, consisted of performing a SVD of the transfer matrix relating pressures at different radii. Singular values smaller than a certain level were truncated in order to remove high order components from the transfer matrix. This procedure is essentially the same as that applied most often in boundary element holography procedures [9]. However, it was found here that all of the other filtering methods examined were more effective than performing a SVD of the transfer matrix.

3.3 Filtering Results

3.3.1 Simulation results

The simulation results in terms of the mean square errors calculated for the ten filtering methods and three sound field cases are given in Table 1. The results presented in Table 1 are the average of the best results obtained by using a specific filtering procedure with multiple sources and random noise. In particular, the results presented in Table 1 were the best results obtained by using a specific filtering method when the filtering level was progressively increased by multiples of 10 dB, except in the cases of spherical harmonic coefficient truncation and SVD filtering, as indicated. The power filtering procedure was found, on average, to result in the smallest projection error.

3.3.2 Experiment results

The sound pressure fields of three different types of sound sources, one loudspeaker, a pair of loudspeakers, and a small air compressor were measured by using the 32 microphone array shown in Fig. 2; measurements were performed at 16 azumuthal angles. Based on

those measurements of sound pressure, both forward and backward projections were performed. The filtering methods described in this article were applied during both forward and backward projections to verify and assess the performance of the various filtering methods. The measurements of a realistic sound source, a small air compressor which is shown in Fig. 3, were of particular interest. Note that the exit of the compressor was aligned with x-axis; i.e., it pointed in the ϕ=0, θ=90 deg. direction. Sound pressure measurements were made at two different radii, 0.240 m and 0.291m. The directly measured pressure on the surface at 0.240 m and the backward projected pressure from the measurement surface at 0.291 m are compared in Figs. 4 and 5 at 60 Hz and 720 Hz. Power filtering with a cutoff level of 40 dB was applied before backward projection. From the results of the spherical holography visualizations, it was clear that the air compressor featured two major source mechanisms. At low frequencies around 60 Hz, the primary sound radiation appeared to be is due to a solid-body vibration of the compressor shell (see Fig. 4). In contrast, at higher frequencies, around 720 Hz, monopole-like pulsating fluid flow at the exit of the air compressor was clearly the primary sound source (see Fig. 5). Sound power calculations were used to show that the low frequency vibration of the compressor radiated very inefficiently compared to the high frequency source [12].

Table 1 Mean square error of various filtering methods

Filtering methods	MSE (%)
Coefficient filtering	4.87
Power filtering	2.65
Pressure filtering	4.94
Spherical harmonic coefficients truncation	6.11
Power filtering truncation	6.19
Coefficient filtering truncation	6.44
Pressure filtering truncation	6.37
SVD filtering without area weighting	6.40
SVD filtering with area weighting	7.31
SVD of transfer matrix	10.10

4. Conclusions

In the work described in this paper, ten different filtering methods were applied to various types of simulated sound fields. It was observed that both the nature of the sound field and the signal-to-noise ratio affect the relative performance of the filtering methods. No single filtering method was found to be the best for all sound sources and signal-to-noise ratios. However if one averages the mean square errors for different sound sources and signal-to-noise ratios, power filtering was found to be the best filtering method among those examined. Even for those cases in which power filtering did not yield the best result, the results of power filtering were not much worse than the results of the best filtering method in each case. In most of the cases, the effect of the superposed random noise in the measured pressure was reduced rather than amplified during power filtering and backward projection.

Spherical holography procedures were also verified experimentally. Reliable results were obtained using the power-filtering algorithm. Thus it was concluded that spherical holography combined with power filtering may prove to be a useful tool for noise source identification. The measurements demonstrated that the procedures described in this article can be used to project sound fields reliably, both forward and backwards, and that the holographic procedures allow particular noise sources to be located and their characteristics to be identified under realistic conditions. The measurements performed on the small compressor, in particular, demonstrated that spherical holography can be a useful tool for noise source identification.

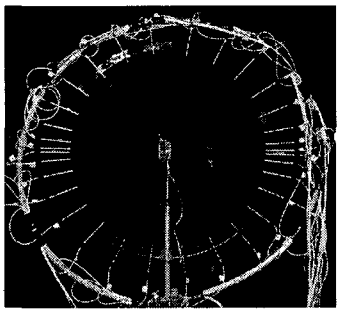

Fig. 2 Microphone array for spherical holography.

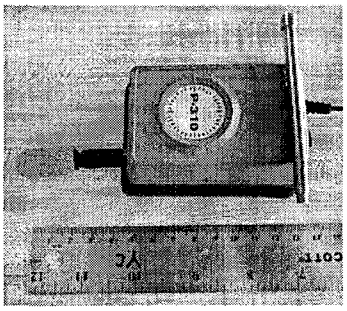

Fig. 3 Small air compressor used in measurements for spherical holography verification.

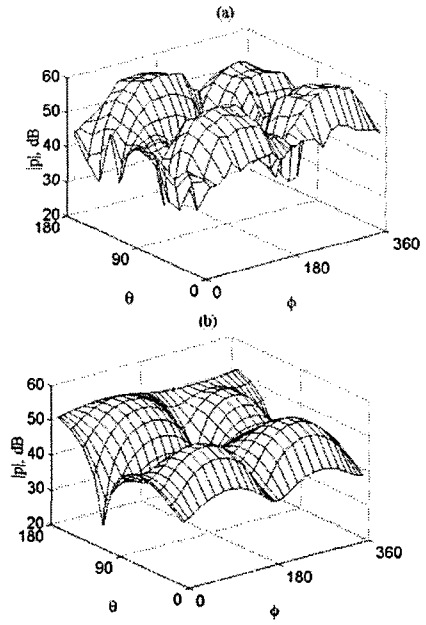

Fig. 4 Air compressor, measured and backward projected pressure, r=0.240m, 60 Hz.
(a) measured pressure, $|p|$
(b) backward projected pressure, $|p|$

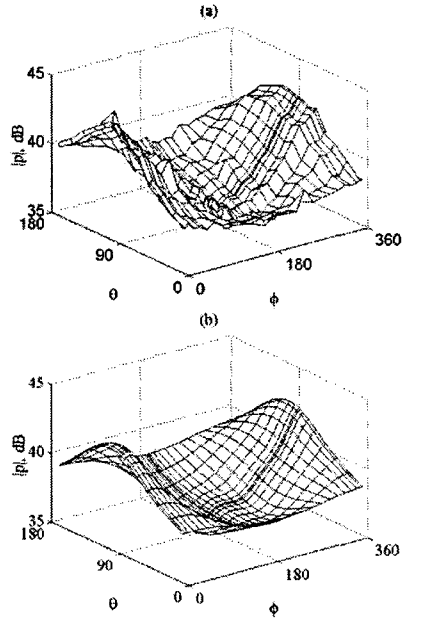

Fig. 5 Air compressor, measured and backward projected pressure, r=0.240m, 720 Hz.
(c) measured pressure, $|p|$
(d) backward projected pressure, $|p|$

References

(1) J. D. Maynard, E. G. Williams, and Y. Lee, 1985, Nearfield Acoustic Holography: I. Theory of Generalized Holography and the Development of NAH. *Journal of the Acoustical Society of America* **78**(4), pp. 1395-1414.

(2) J. Hald and K. B. Ginn, 1989, Vehicle Noise Investigation Using Spatial Transformation of Sound Fields, *Sound & Vibration,* **23**(4), pp. 38-45.

(3) E. G. Williams, H. D. Dardy, and K. B. Washburn, 1987, Generalized Nearfield Acoustic Holography for Cylindrical Geometry: Theory and Experiment, *Journal of the Acoustical Society of America* **81**(2), pp. 389-407.

(4) A. Sarkissian, C. F. Gaumond, E. G. Williams, 1993, and B. H. Houston, Reconstruction of the Acoustic Field over a Limited Surface Area on a Vibrating Cylinder, *Journal of the Acoustical Society of America* **93**(1), pp. 48-54.

(5) E. G. Williams, 1999, *Fourier Acoustics: Sound Radiation and Nearfield Acoustical Holography*, Academic Press, San Diego.

(6) L. A. DeVries, 1994, Acoustical Holography in Spherical Coordinates for Noise Source Identification, M.S.M.E. Thesis, Purdue University.

(7) L. A. DeVries, J. S. Bolton, and J. C. Lee, 1994, Acoustical Holography in Spherical Coordinates for Source Identification, *Proceedings of NOISE CON 94*, pp. 935-938.

(8) G. Weinreich and E. B. Arnold, 1980, Method for Measuring Acoustic Radiation Fields, *Journal of the Acoustical Society of America* **68**(2), pp. 404-411.

(9) J.-G. Ih, S.-C. Kang, S.-J. Kim, K.-S. Kang, 1998, "Reconstruction of the Vibro-acoustic Field on the Surface of the Refrigerator Compressor by using the BEM-based Acoustic Holography," International Compressor Engineering Conference 98, Purdue University, pp. 525-529.

(10) F. Laville, M. Sidki, and J. Nicolas, 1992, Spherical Acoustical Holography Using Sound Intensity Measurements: Theory and Simulation, *Acustica* **76**, pp. 193-198.

(11) J. C. Lee, 1996, Spherical Acoustical Holography of Low-Frequency Noise Source, *Applied Acoustics* **48**(1), pp. 85-95.

(12) Y. T. Cho, 2002, Spherical Acoustical Holography, M.S.M.E. Thesis, Purdue University.